Desalination and Water Treatment
www.deswater.com

doi: 10.5004/dwt.2020.25190

183 (2020) 346–354
April

Numerical simulation of chemical reaction – solute transport coupling model of 2,4-DCP in groundwater

Yongxiang Zhang[a,*], Xuezheng Huang[a,b], Weichun Gao[a,c], Youhao Wang[a], Shan Chang[a]

[a]*School of Architecture and Civil Engineering, Beijing University of Technology, Beijing 100124, China, Tel. +86-010-67396090; email: yxzhang@bjut.edu.cn (Y. Zhang), Tel. +86-17810290678; email: 58626472@qq.com (X. Huang), Tel. +86-18810372310; email: gaoweichun_01@126.com (W. Gao), Tel. +86-18813085024; email: wyhzmm@sina.com (Y. Wang), Tel. +86-15810417569; email: xxxcoarse sand hine@163.com (S. Chang)*
[b]*School of Civil Engineering, Nanyang Institute of Technology, Nanyang 473004, Henan Province, China*
[c]*Shenyang University of Technology, Shenyang,110870, Liaoning Province, China*

Received 21 May 2019; Accepted 15 November 2019

ABSTRACT

A permeable reactive barrier (PRB) remediation test trough with coarse sand-supported zero-valent iron (ZVI) composite filler was designed and built. Considering the convection-dispersion and chemical reaction of 2,4-dichlorophenol (2,4-DCP) in groundwater, a coupled model of chemical reaction and solute transport of 2,4-DCP was built. The adsorption kinetics data of 2,4-DCP were fitted, the results showed the pseudo-second-order kinetic model could better describe 2,4-DCP adsorption process than the pseudo-first-order kinetic model. The model parameters were determined by static adsorption test and continuous flow dynamic tracer test. Compared with the linear model and the Langmuir model, the Freundlich model fits better with the adsorption test data, it shows that the adsorption of 2,4-DCP by coarse sand and coarse sand-supported ZVI filler was more in line with the Freundlich model. A Freundlich model showed a satisfactory fit to the equilibrium adsorption data with a correlation coefficient $R^2 = 0.968$ for coarse sand and $R^2 = 0.954$ for coarse sand-supported ZVI. The adsorption coefficient K_F of 2,4-DCP on coarse sand and coarse sand-supported ZVI are 4.456×10^{-6} and 0.00846 respectively, the dispersion coefficient is 0.345 cm^2/min, the porosity is 0.38, the specific yield is 0.1, the permeability coefficient is 4.15×10^{-2} cm/s, and the seepage velocity is 1.245×10^{-4} cm/s. The FEMWATER software and the TOUGHREACT software are used to calculate the coupling model to simulate the migration and transformation process of 2,4-DCP in groundwater. The results show that the calculated values by software TOUGHREACT do not agree well with the measured values for the failure zone of composite filler, the values calculated by software FEMWATER has better fitting effect with the measured values.

Keywords: Coarse sand; Zero-valent iron; Simulation; Coupling model; Groundwater

1. Introduction

2,4-dichlorophenol (2,4-DCP), as one of the chlorophenols, has strong toxicity, carcinogenicity, and mutagenicity. It is difficult to biodegrade and easy to accumulate in animals. It is widely used in the production of wood preservatives, herbicides, insecticides, etc. Once entering the environment, it accumulates and imposes long-term adverse effects on human health and the ecological environment [1–3]. Therefore, it is listed as a priority pollutant by US Environmental Protection Agency (EPA) and European Environment Agency (EEA) [4] and is blacklisted as a priority pollutant in water by China National Environmental Monitoring Center (CENMC). It is an important and urgent

* Corresponding author.

task to study the removal of organic pollutants, especially chlorinated compounds of groundwater [5].

The conventional technology used to remediate contaminated groundwater has been the 'pump-and-treat' (P&T) systems. However, clean-up goals have hardly been met with this technique [6]. Thus a large number of research papers on pollutant removal in groundwater have been published in the past 30 years. Permeable reactive barriers (PRBs) are a low-cost in-situ remediation technology for groundwater pollution, which was proposed by the US Environmental Protection Agency in the late 1980s. Its basic principle is to insert reactive materials with physical, chemical, biological functions or their combination functions into the underground aquifer in a certain geometric form, and the upstream contaminants are intercepted and treated in the barriers as the plume flows through it under the influence of the natural hydraulic gradient. As contaminated water passes through the reactive zone of the PRBs, the contaminants are either immobilized or chemically transformed to a more desirable (e.g., less toxic, more readily biodegradable, etc.) state via processes such as adsorption, precipitation, denitrification and biodegradation [7].

Since the invention of PRBs in the early 1990s, granular activated carbon, zero-valent iron (ZVI), red mud, fly ash, peat, activated sludge, tree leaves, steel fibers from tires, blast furnace slag, steel slag dust, plant shell and weed, bone char, non-living biomass, maize cob, etc., are examples for materials that can be used in the PRB for containment of the pollutants [8]. The most common reactive materials are ZVI [9,10]. In June 1996, a PRB was established at the contaminated site of the North Carolina Coast Guard Airport [11], TCE decreased from 6 to 0.005 mg/L. If the system operated continuously for 20 years, it would save 4 million dollars compared with the traditional pump & treat system. Parbs et al. [12] noted that soluble carbonates affected the long-term removal of TCE by ZVI. Carbonate and bicarbonate ions accelerated the corrosion of ZVI. At the same time, due to the adsorption and precipitation of carbonate on the surface of ZVI in this buffer system, the active sites of ZVI were reduced. Li et al. [13] noted the removal rate of PCE by ZVI can reach more than 80%. The removal of PCE by ZVI treatment system has both chemical reaction and physical adsorption. By 2010, there will be more than 200 ZVI PRB projects worldwide, including more than 150 commercial remediation projects [14].

In 1994, Gillham et al. [15] proposed for the first time that ZVI can be used for in-situ remediation of groundwater and chlorinated organic compounds can be effectively dechlorinated by metallic iron. Since then ZVI gained increasing attention due to its low toxicity, low price, easy operation and less secondary pollution to the environment [16]. Especially in the past decade, nanoscale zero-valent iron (nZVI) has been extensively and deeply studied in in-situ groundwater remediation due to its large specific surface area and strong reductive activity [17–21]. However, the application of nZVI is restricted by its easy passivation, easy agglomeration and poor transport [22]. Therefore, the introduction of materials with low reactivity, such as sand or natural minerals, to fix ZVI is an effective measure to improve the permeability of PRB. It can improve the specific surface area, adsorption capacity and pollutant removal efficiency of ZVI [23]. The research group prepared and characterized coarse sand-supported ZVI composite filler and the result indicates that 2,4-DCP degradation by coarse sand-supported ZVI filler follows the pseudo-second-order kinetic model and the degradation effect is remarkable. The related research results can be seen in the literature [24].

With the development of computer technology, numerical simulation of pollutant transport and groundwater flow have gradually become an important method to study the effect of groundwater remediation due to its flexibility, effectiveness and low cost. The numerical simulation of contaminant transport in the PRB process is an important means to evaluate the effect of PRB on the remediation of contaminated groundwater [25]. Weber et al. [26] used an enhanced version of MIN3P to simulate dominating processes in chlorinated hydrocarbons treating ZVI PRBs. The results of model of field site demonstrated that temporarily enhanced groundwater carbonate concentrations caused an increase in gas phase formation due to the acceleration of anaerobic iron corrosion. Benner et al. [27] evaluated and analyzed the performance of a permeable reactive barrier, designed to remove metals and generate alkalinity by metal sulfide precipitation, by means of chemical analysis coupled with geochemical speciation modeling using MINTEQA2 code. They reported that the dominant changes in water chemistry in the barrier and down-gradient aquifer can be attributed to bacterially mediated sulfate reduction. Deng et al. [28] constructed a 3D coupling model of groundwater seepage and nitrate pollution migration by numerical analysis method and simulated the nitrate remediation effect of Fe0-PRB in groundwater by GMS software. The simulation results show that the PRB of 6 m thick and 4 m thick can degrade the nitrate from 600 mg/L upstream of PRB to 0.52 and 1.71 mg/L respectively. Jeen et al. [29] applied the MIN3P model to simulate the degradation of TCE by ZVI in an unsaturated porous medium in PRBs and compared it with the observed result of a long-term column test. The model successfully demonstrates the dynamic change of iron reactivity and contaminant treatment effect, and the research makes remarkable headway in predicting the long-term behavior of Fe-PRB. Eljamal et al. [30] established a one-dimensional solute transport model coupled with chemical reactions to simulate the process of removal of trivalent arsenic by ZVI in PRBs column experiments. The simulation results show that the adsorption rate of pentavalent arsenic is faster than that of trivalent arsenic. ZVI can be used as an effective reagent for in situ arsenic remediation in groundwater. There are a great number of research publications about PRBs simulation with the solute transport model [31–33], and most of them focus on heavy metal simulation. Up to now, the simulation of solute transport for chlorophenols in the PRB system has rarely been reported in the literature.

In the paper, considering the convection-dispersion and chemical reaction of 2,4-DCP in groundwater, the chemical reaction-solute transport model of 2,4-DCP in PRB test trough is constructed. The model parameters are determined by static test, and the concentration of 2,4-DCP at PRB outlet is determined by continuous flow dynamic PRB test. The simulated values were calculated by TOUGHREACT software and compared with the measured values to verify the correctness of the coupled chemical reaction-solute

transport model, reveal the migration and transformation laws of 2,4-DCP, simulate the remove effect of PRB technology on 2,4-DCP, and provide effective data and theoretical support for the PRB technology to remove chlorophenol compounds in the field.

2. PRB test device with coarse sand-supported ZVI composite filler

2.1. Construction of PRB remediation test device

As shown in Fig. 1, the PRB test device with coarse sand-supported ZVI composite filler is composed of PRB remediation test trough, water distribution tank, gas intake tank, and gas collector. The PRB remediation test trough is a plexiglass cuboid. The flow rate of the inlet and outlet can be adjusted by the electromagnetic diaphragm metering pump.

The PRB remediation test trough consists of water trough I, sand trough II and reaction medium trough III. The water trough, 20 cm × 40 cm × 80 cm, with water inlet and outlet adjustable by valves, is used to simulate groundwater level; the sand trough, 25 cm × 40 cm × 80 cm, with 1 to 2 mm coarse sand as filler and filling height of 72 cm, is used to simulate groundwater aquifer; the reaction medium trough, 30 cm × 40 cm × 80 cm, with coarse sand-supported ZVI composite as filler (refer to literature [24] for detailed preparation method) and filling height of 72 cm, is used to simulate PRB for treatment of organic contaminants in groundwater. In the sand trough and reaction medium trough, there are 3 × 4 sampling holes with an inner diameter of 2 cm respectively.

The water used in the test is untreated groundwater taken from a deep well in Beijing. The concentration of the prepared 2,4-DCP inflow water is 20 mg/L and the feeding mode is continuous water feeding.

2.2. Debugging and operation of PRB remediation test device

2.2.1. Debugging of PRB remediation test device

Firstly, water is injected slowly through the liquid flowmeter from the bottom of the test trough to exhaust and saturate the test trough. When the water level in the test trough reaches 3–4 cm high from the bottom of the coarse sand layer and the reaction medium layer, stop water injection and keep it stable for a certain time to ensure complete exhaust. When the water level in the test trough is stable, the water level will be raised by 3 to 4 cm by water injection until the sand layer and the reaction medium layer in the test trough are immersed. Finally, after the test trough is fully saturated, close the bottom water injection valve of the test trough, and open the inlet and outlet solenoids respectively for groundwater lever regulation. When the water level difference between the two sides is 3 mm, the hydraulic gradient is 3‰.

2.2.2. Operating conditions of PRB remediation test device

PRB remediation test trough is shaded with cellophane and filled with argon to create a closed groundwater reduction environment, avoiding photolysis of 2,4-DCP and oxidation of reaction medium. Continuous automatic water

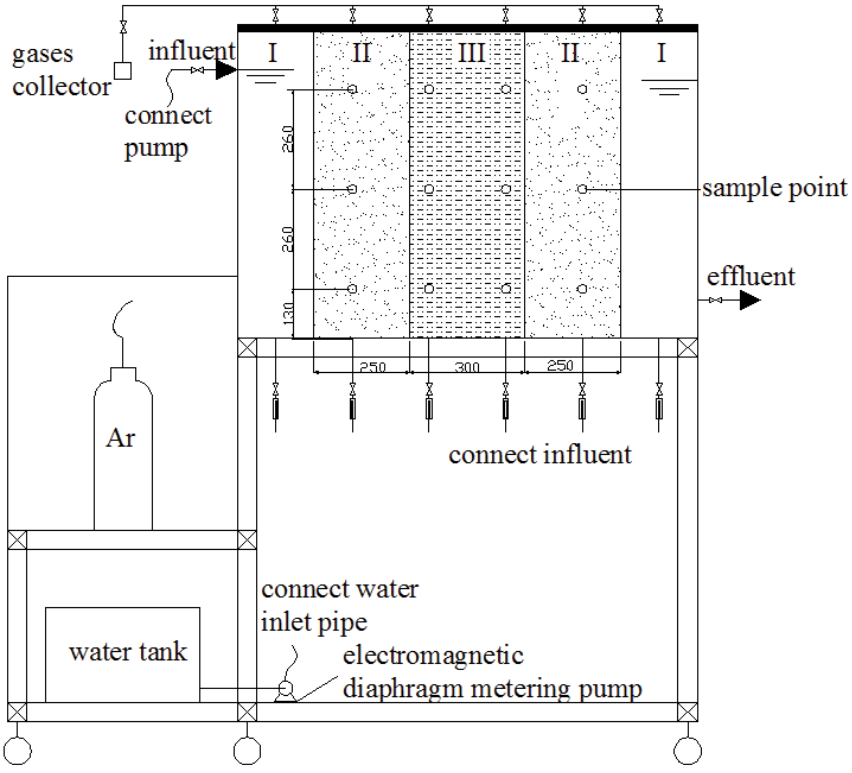

Fig. 1. PRB remediation test device. I. Water trough; II. Sand trough; and III. Reaction medium trough.

intake of the test trough is achieved by metering pump. The influent concentration of 2,4-DCP was 20 mg/L, the influent velocity was 1.2 L/h and the influent volume was 0.0288 m^3/d. The groundwater level of the PRB remediation test trough is controlled at 67 cm. The concentration of 2,4-DCP was analyzed at 12 sampling holes and outlets. At the same time, the changes of pressure measuring tubes in 12 holes were monitored to determine the groundwater level in the test trough. When the concentration of 2,4-DCP in the effluent reaches 20 mg/L, the test is stopped.

2.2.3. Adsorption kinetics of 2,4-DCP

For the core-shell structure of coarse sand-supported ZVI composite in batch experiments, concentration-time curve of 2,4-DCP in groundwater is presented in Fig. 2.

It can be seen from Fig. 2 that the concentration of 2,4-DCP decreases first, then rises, and then decreases continuously. It shows that the complex process of degrading 2,4-DCP by ZVI on the surface of composite fillers includes adsorption, desorption and reductive dechlorination of 2,4-DCP [24]. Firstly, The Si component in the composite material has a great influence on the adsorption. Si can improve the surface hydrophobicity of composite materials, which leads to the preferential adsorption of organic compounds [34]. At this stage, 2,4-DCP is adsorbed by a large amount of ZVI and sodium alginate in the composite filler. Secondly, there is a complex competitive process between adsorption and desorption. Some adsorbed 2,4-DCP is desorbed from the surface of composite fillers [35]. Finally, the dynamic equilibrium between adsorption and desorption was established. Therefore, the reduction dechlorination reaction was the main route in the degradation of 2,4-DCP by composite fillers. The pseudo-first-order kinetic model was described as follows.

$$\ln\left(q_e - q_t\right) = \ln q_e - k_1 t \tag{1}$$

The pseudo-second-order kinetics model should be described as follows.

$$\frac{1}{q_e - q_t} = \frac{1}{q_e} + k_2 t \tag{2}$$

where k_1 (min^{-1}) and k_2 (g mg^{-1} h^{-1}) is the adsorption rate constant. q_e and q_t (mg g^{-1}) are the amounts of 2,4-DCP adsorbed over composite at equilibrium and time t (min), respectively.

The data of 2,4-DCP adsorption kinetics are fitted by pseudo-first-order kinetics model and pseudo-second-order kinetics model. The adsorption rate constants and adsorption capacity are shown in Table 1.

From Table 1, we can see that the correlation coefficient R^2 of the pseudo-second-order kinetics model is closer to 1 than that of the pseudo-first-order kinetics model. It implies that adsorption of 2,4-DCP follows a second-order kinetics model and the control mechanism of adsorption reaction is chemical adsorption of surface reaction. When chlorinated organic compounds are treated with ZVI, oxidation of ZVI and Fe(II) provide electrons for dechlorination [36].

$$Fe + H_2O \rightarrow Fe^{2+} + H_2 + 2OH^- \tag{3}$$

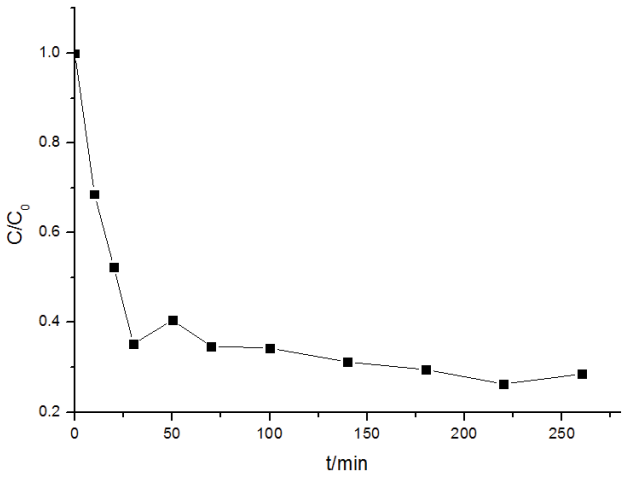

Fig. 2. Degradation process of 2,4-DCP in groundwater.

Table 1
Adsorption kinetic parameters of 2,4-DCP in groundwater

Pseudo-first-order			Pseudo-second-order		
q_e (mg g^{-1})	k_1 (min^{-1})	R^2	q_e (mg g^{-1})	k_2 (g mg^{-1} h^{-1})	R^2
0.0078	0.06188	0.9670	0.5050	0.2149	0.9972

$$Fe + R - Cl + H^+ \rightarrow Fe^{2+} + R - H + Cl^- \tag{4}$$

$$2Fe^{2+} + R - Cl + H_2O \rightarrow 2Fe^{3+} + R - H + Cl^- \tag{5}$$

3. Conceptual model of 2,4-DCP chemical reaction-solute transport

3.1. Model conceptualization

In this study, the PRB remediation test trough is taken as the research object, and its hydrogeological conditions are simple. The filling media for sand trough and reaction medium trough are coarse sand and coarse sand-supported ZVI composite filler respectively, which can generalize the groundwater flow in the PRB remediation test trough into the homogeneous, isotropic and steady phreatic water flow. Considering that the water surface of the PRB test trough is relatively flat and the flow is horizontal, the vertical and transverse components of seepage velocity can be neglected, so it can be simplified to one-dimensional flow.

In the simulation, according to the distribution of PRB reaction, it is determined that the simulation range of the PRB test trough with 80 cm length, The water trough at either side of the PRB test trough is generalized as the boundary of fixed water level, and the top, bottom and side boundaries of the test trough are generalized to zero flux and concentration boundaries.

According to continuous-flow test, the left water trough is generalized as the boundary of fixed concentration and fixed head, the right water trough is generalized as the

boundary of fixed concentration and fixed head, and the groundwater and 2,4-DCP are sourced from the left water trough through lateral feeding based on model input.

The simulation range is divided into coarse sand range and reaction medium range. For grid cell generation in the coarse sand range, one grid cell is generated for every 2 cm, so there are 26 grid cells in coarse sand range in total at both sides; For reaction medium range which is the primary range for 2,4-DCP reaction, one grid cell is generated for every 1 cm, so there are 30 grid cells in reaction medium range; therefore, there are 56 grids in the simulation range. Because TOUGHREACT is capable of adaptive time-stepping, the time step is determined as 1 h, and the simulation lasts for 50 d.

3.2. Numerical groundwater flow model

Based on the conceptual model of groundwater and the determination of initial and boundary conditions of the PRB simulation range, the numerical groundwater flow model is constructed as follows:

$$\begin{cases} \dfrac{\partial}{\partial x}\left(K(H-Z)\dfrac{\partial H}{\partial x}\right)-W(t)=\mu\dfrac{\partial H}{\partial t} \\ H(x)\big|_{t=0}=H_0(x), \qquad 0\le x\le 0.8 \\ H(x,t)\big|_{\Gamma_1}=H_1(x,t), \qquad t>0 \end{cases} \tag{6}$$

where x is the direction along the water flow direction, t is time, K is permeability coefficient, Z is groundwater floor elevation, H is groundwater level, $W(t)$ is source-sink term, μ is specific water yield, $H(x)\,|_{t=0}$ is the water head of the grid when $t = 0$, $H_0(x)$ is the water head of grid point, Γ_1 is the boundary of fixed water level of the PRB remediation test trough, $H(x,t)\big|_{\Gamma_1}$ is the water head value at boundary at the time t, and $H_1(x,t)$ is the elevation of grid.

3.3. Model of solute transport

Based on the full consideration to the joint influence of multiple factors including flow, hydrodynamic dispersion, adsorption, the coupling model of 2,4-DCP transport in groundwater is constructed as follows:

$$\begin{cases} \dfrac{\partial C}{\partial t}=\dfrac{\partial}{\partial x}\left(D\dfrac{\partial C}{\partial x}\right)-\dfrac{\partial}{\partial x}(v_x C)+\dfrac{q_s}{n}C_s-A \\ C(x,0)=C_0(x), \qquad 0\le x\le 0.8 \\ C(x,t)\big|_{\Gamma_1}=C_1(x,t), \qquad t>0 \end{cases} \tag{7}$$

where C is the concentration of 2,4-DCP in groundwater, C_0 is the initial concentration of 2,4-DCP in groundwater and $C_0 = 0$ in the research, C_1 is the Dirichlet boundary concentration of 2,4-DCP in groundwater, coarse sand is the concentration of 2,4-DCP in source-sink term, D is dispersion coefficient, v_x is the horizontal flow velocity of groundwater, n is porosity, q_s is volume flow rate per unit volume, $\dfrac{\partial}{\partial x}\left(D\dfrac{\partial C}{\partial x}\right)$ is the hydrodynamic dispersion term, $\dfrac{\partial}{\partial x}(v_x C)$ is the convection term, $\dfrac{q_s}{n}C_s$ is the source and sink items, A is the adsorption item.

3.4. Determination of parameters for chemical reaction – solute transport coupling model

3.4.1. Determination of adsorption coefficient

Prepare two groups of conical flasks (each group has seven flasks), fill sterilized coarse sand filler and coarse sand-supported ZVI composite filler into each group of flasks, add 100 mL 2,4-DCP solute prepared with pure water, with concentration of 1, 2, 5, 10, 12, 15 and 20 mg/L, respectively to the flasks, mix filler and solution, put the flasks in thermostatic oscillator for reaction until reaching equilibrium, and take supernatant to analyze the concentration of 2,4-DCP.

The adsorption capacity of filler can be calculated according to the following formula:

$$q_e=\frac{(C_0-C_e)}{W}V \tag{8}$$

where q_e is the adsorption capacity of filler for 2,4-DCP adsorption, mg/g; C_0 (mg/L) is the initial concentration of 2,4-DCP in solution, mg/L; C_e (mg/L) is the concentration of 2,4-DCP in adsorption equilibrium, V(L) is solution volume, W(g) is the mass of filler.

The common isothermal adsorption models include linear adsorption model, Freundlich adsorption model, Langmuir adsorption model, etc. The linear adsorption model is:

$$q_e=K_d C_e \tag{9}$$

The Freundlich adsorption model formula is:

$$q_e=K_F C_e^{1/n} \tag{10}$$

The Langmuir adsorption model is:

$$q_e=\frac{q_m K_L C_e}{1+K_L C_e} \tag{11}$$

where C_e and q_e are the concentration (mg L^{-1}) and adsorption capacity (mg g^{-1}) at equilibrium, q_m (mg g^{-1}) is the maximum adsorption capacity of the adsorbent and K_L (L mg^{-1}) is the Langmuir constant, K_F (mg g^{-1} (mg/L)$^{n-1}$) and K_d (L g^{-1}) are the constants of Freundlich and linear models, respectively; n is the exponent of Freundlich model.

The test data are fitted respectively according to the three models, and the calculation results are shown in Table 2.

From Table 2 it is obvious that when the Freundlich adsorption model is applied for composite filler, R^2 is closest to 1, which indicates that the adsorption type of the composite

Table 2
Parameters for the linear model, Langmuir model and Freundlich models

Adsorption model	Parameter	Coarse sand	Coarse sand-supported ZVI composite
Linear model	K_d	4.004E-4	0.0029
	R^2	0.847	0.898
Freundlich model	K_F	4.456E-6	0.00846
	n	0.381	1.827
	R^2	0.968	0.954
Langmuir model	K_L	9.094E-6	0.238
	q_m	37.039	0.0395
	R^2	0.804	0.952

filler for 2,4-DCP adsorption is Freundlich adsorption, and the corresponding adsorption coefficient K_F is 0.00846.

3.4.2. Determination of porosity and specific water yield

In the research, the parameters such as porosity and specific water yield are determined through laboratory tests based on the volumetric method. The calculation of porosity n is as shown by Eq. (12):

$$n = \frac{V_1}{V_3} \tag{12}$$

In Eq. (12), V_1 is the volume of water when the pores of the coarse sand sample are filled with water; V_2 is the volume of free-outflowing water; V_3 is the total volume of coarse sand sample.

The calculation of specific water yield μ is as shown by Eq. (13):

$$\mu = \frac{V_2}{V_3} \tag{13}$$

In Eq. (13), V_2 is the volume of free-outflowing water; V_3 is the total volume of coarse sand sample. The test-based determined porosity is 0.38 and the specific water yield is 0.1.

3.4.3. Determination of permeability coefficient

Permeability coefficient is an indicator of expressing rock permeability and one of the important hydrogeological parameters about aquifer property. From Darcy law, it is known that:

$$Q = K\frac{\Delta H}{l}\omega \tag{14}$$

where Q is seepage flow; ω is the seepage section area; ΔH is water head difference; l is the distance between sections; K is the permeability coefficient.

According to the calculation based on the test data about degradation of 2,4-DCP in groundwater by coarse sand-supported ZVI PRB, the seepage flow is 1.2 L/h, the PRB seepage section area (ω) is 0.4 × 0.67 m^2, the hydraulic slope is 3%, and the permeability coefficient is 4.15 × 10^{-2} cm/s. Through calculation based on Darcy law, the seepage velocity is 1.245 × 10^{-4} cm/s.

3.4.4. Determination of hydrodynamic dispersion coefficient

Hydrodynamic dispersion coefficient is an important hydrogeological parameter for characterizing the transport of solute in groundwater. It characterizes the ability of a porous medium to disperse a dissolved substance at a certain flow rate. To obtain the hydrodynamic dispersion coefficient of the porous medium in groundwater is a prerequisite for introducing the mathematical convection-dispersion model. In the research, the hydrodynamic dispersion coefficient is determined by the breakthrough curve, the tracer is a NaCl solution, and the dosing mode is continuous dosing. Refer to the literature [32] for detailed test steps. Through test determination and data calculation, the dispersion coefficient is 0.345 cm/s, and the seepage velocity is 2.2 × 10^{-4} cm^2/min.

3.4.5. Chemical composition of initial water

The initial water is prepared with groundwater taken from a deep well in Beijing City and added with a 20 mg/L 2,4-DCP solution. The concentration measurement of the nine key components in groundwater, namely K^+, Na^+, Ca^{2+}, Mg^{2+}, Fe^{2+}, HCO_3^-, Cl^-, SO_4^{2-}, and NO_3^-, shows that the corresponding concentration is 1.79, 14.4, 61.7, 26.5, 0.127, 224.6, 21.3, and 43.9 mg/L, respectively.

3.4.6. Composition of coarse sand-supported ZVI composite

Scanning electron microscopy (SEM) and energy-dispersive X-ray spectroscopy (EDS) analysis of coarse sand-supported ZVI composite filler were carried out. The SEM and EDS photographs are detailed in reference [24]. Coarse sand-supported ZVI composite filler belongs to a core-shell structure, which is a polymer formed by a single irregular particle. Sodium alginate encapsulates ZVI in the form of a shell. There is a wide pore distribution in the composite filler, which provides a convenient environment for ZVI powder reacting with 2,4-DCP in groundwater. The energy spectrum analysis of a micro-area of the composite filler shows that the composite filler is mainly composed of C, O, Fe, and Ba elements, accounting for 97.1% of the total weight, Other trace elements are Si, S, Cl, and Ca. The contents of the elements are shown in Table 3. The presence of Ba in EDS analysis is mainly due to the use of barium chloride in the preparation of composite fillers, and the main reason for the existence of Si is that the iron powder purchased contains Si impurities.

3.5. Model debugging and operation

Run software TOUGHREACT, input the model parameters as shown in Table 4, make a model-based calculation and conduct a comparative analysis of the calculation results and test results, and repeatedly adjust the parameters related to adsorption coefficient in the database until the

Table 3
EDS analysis results of coarse sand-supported ZVI composite

Element/ atomic layer	Weight percentage (%)	Atomic percentage (%)
C/K	6.97	14.83
O/K	37.30	59.59
Si/K	1.19	1.09
S/K	0.88	0.70
Cl/K	0.48	0.34
Ca/K	0.36	0.23
Fe/K	49.32	22.57
Ba/L	3.51	0.65
Total	100.00	100.00

Table 4
Model parameters

Permeability coefficient (m/d)	35.86
Bulk density	2,000
Bending degree	1.0
Transverse dispersion (m)	0.26
Longitudinal dispersion (m)	0.026
Retardation factor	0.3
Porosity	0.38

model-based calculated values and the test-based measured values are well fitted.

3.6. Validation of model-based calculation results

Obtain the simulated values of the chemical reaction-solute transport coupling model constructed through software TOUGHREACT, sample the water respectively at sampling hole 2–2 in the reaction medium-range and outlet during testing, measure 2,4-DCP concentration and obtain the measured values, and plot the simulated values and measured valves of 2,4-DCP concentration at different reaction time, as shown in Figs. 3 and 4.

It is known from Figs. 3 and 4 that, as water sample continuously flows into the reaction medium tank, 2,4-DCP concentration in the reaction medium-range gradually increases and tends to stabilize from the tenth day, agreeing well with the simulated values, and that in the outlet gradually increases and tends to stabilize from the twentieth day, agreeing well with the simulated values. In addition, it is also obvious that within the time range when the measured values of 2,4-DCP concentration are small, the fluctuation is large, showing irregularity; the reason is that many factors are influencing 2,4-DCP concentration measurement, which interferes with the accuracy of measured results. Besides, it can be seen that 2,4-DCP concentration increases sharply after 40 d and reaches the initial concentration of 20 mg/L, which is not in good agreement with the simulation value. The reason is that with the reaction proceeding, the passivation of ZVI composite filler

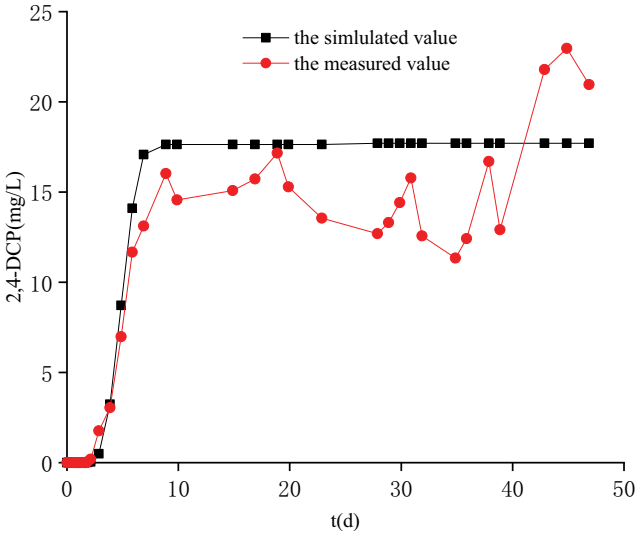

Fig. 5. The fitting curve for measured and simulated values by software TOUGHREACT at sampling hole 2–2.

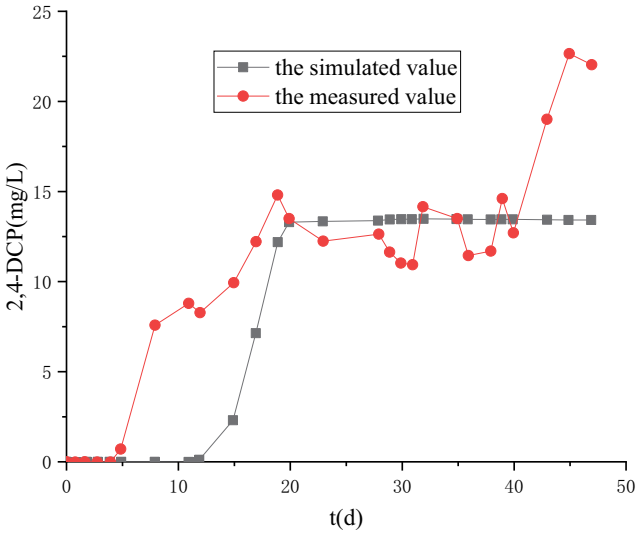

Fig. 4. The fitting curve for measured and simulated values by software TOUGHREACT in the outlet.

with coarse sand leads to the decrease of reaction activity. In addition, the long-term precipitation of reactive minerals on the surface of the filler has adverse effects on the permeability of the reaction medium, which makes the composite filler lose the function of degrading 2,4-DCP so that the concentration of 2,4-DCP at the outlet rises to the import.

To achieve a better simulation effect, the FEMWATER module in GMS software is used to calculate the model based on a chemical adsorption reaction the solute transport coupling model. The simulation was carried out in two periods, that is, from 2,4-DCP concentration rising rapidly to stable period (1–40d, retardation factor is 0.3) and composite filler losing utility period (41–48 d, retardation factor is 0). The fitting effect of 2,4-DCP simulated value and measured value at sampling hole 2–2 of the reaction medium-range calculated by FEMWATER software is shown in Fig. 5. As a whole, it

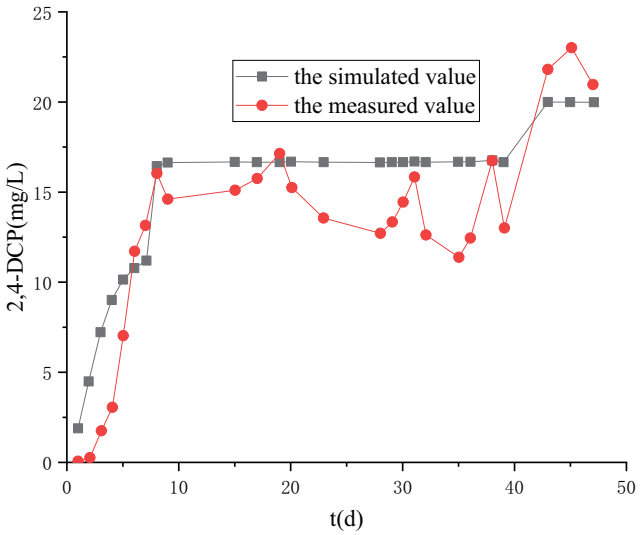

Fig. 5. The fitting curve for measured and simulated values by software FEMWATER at sampling hole 2–2.

can be seen that the measured value and simulated value of 2,4-DCP are in good agreement.

4. Conclusion

- The research group designed and built a PRB test device with course sand-supported ZVI composite filler, successfully simulated the treatment of 2,4-DCP in groundwater with PRB technology using continuous-flow operation mode, constructed a 2,4-DCP chemical reaction-solute transport coupling model, determined the model parameters by static test calculated the coupling model by running TOUGHREACT and FEMWATER software and validate the coupling model with the measured test data.
- The kinetic experimental data show that the adsorption reaction of 2,4-DCP follows a second-order kinetic model. Adsorption of 2,4-DCP by coarse sand and coarse sand-supported ZVI fillers accords with Freundlich adsorption equation by fitting the adsorption equilibrium experimental data, their adsorption coefficients were 4.456×10^{-6} and 0.00846, respectively; the dispersion coefficient value was 0.345 cm^2/min by dispersion test, the porosity was 0.38, the specific yield was 0.1. According to Darcy's law, the seepage coefficient is 4.15×10^{-2} cm/s and the seepage velocity is 1.245×10^{-4} cm/s.
- The calculation results by software TOUGHREACT show that TOUGHREACT cannot fit well for the failure zone of composite filler. The calculation results by software FEMWATER show that the water level in the PRB reactor is stable and the change is not obvious. 2,4-DCP increases gradually along the direction of pushing flow with time; 2,4-DCP rises rapidly to the concentration stable period and the useless period of composite packing have a good fit between the simulated and measured values.
- The coupled model of 2,4-DCP chemical reaction-solute transport can be used to predict the long-term reactive transport process of 2,4-DCP in the PRB process and to evaluate the effect of PRB on remediation of polluted groundwater. The concentration changes of 2,4-DCP at different locations in PRB are simulated and the life of PRB is predicted, which provides technical guidance and scientific basis for the design of PRB.

Acknowledgments

This work is supported by the Integration and demonstration of the technology research and development of Beijing Tianjin Hebei water resources security protection technology (2016YFC0401404). National key research and development program in 2016.

References

[1] Z. Zhang, N. Cissoko, J.J. Wo, X.H. Xu, Factors influencing the dechlorination of 2,4-dichlorophenol by Ni–Fe nanoparticles in the presence of humic acid, J. Hazard. Mater., 165 (2009) 78–86.
[2] H.R. Pouretedal, E. Saedi, Dechlorination of 2,4-dichlorophenol by zero-valent iron nanoparticles impregnated MCM-48, Int. J. Ind. Chem., 5 (2014) 77–83.
[3] M. Raoov, S. Mohamad, M.R. Abas, Removal of 2,4-dichlorophenol using cyclodextrin-ionic liquid polymer as a macroporous material: characterization, adsorption isotherm, kinetic study, thermodynamicoarse sand, J. Hazard. Mater., 263 (2013) 501–516.
[4] J. Xu, X. Lv, J. Li, Y. Li, L. Shen, H. Zhou, X. Xu, Simultaneous adsorption and dechlorination of 2,4-dichlorophenol by Pd/Fe nanoparticles with multi-walled carbon nanotube support, J. Hazard. Mater., 225 (2012) 36–45.
[5] Y. Li, Y. Zhang, J. Li, G. Sheng, X. Zheng, Enhanced reduction of chlorophenols by nanoscale zerovalent iron supported on organobentonite, Chemosphere, 92 (2013) 368–374.
[6] A.D. Henderson, A.H. Demond, Long-term performance of zero-valent iron permeable reactive barriers: a critical review, Environ. Eng. Sci., 24 (2007) 401–423.
[7] F. Obiri-Nyarko, S.J. Grajales-Mesa, G. Malina, An overview of permeable reactive barriers for in situ sustainable groundwater remediation, Chemosphere, 111 (2014) 243–259.
[8] S. Maitra, Permeable reactive barrier: a technology for groundwater remediation – a mini review, Biodegradation, 80 (2019) 203–216.
[9] H.R. Pouretedal, E. Saedi, Dechlorination of 2,4-dichlorophenol by zero-valent iron nanoparticles impregnated MCM-48, Int. J. Ind. Chem., 5 (2014) 77–83.
[10] M. Raoov, S. Mohamad, M.R. Abas, Removal of 2,4-dichlorophenol using cyclodextrin-ionic liquid polymer as a macroporous material: characterization, adsorption isotherm, kinetic study, thermodynamicoarse sand, J. Hazard. Mater., 263 (2013) 501–516.
[11] F.I. Khan, T. Husain, R. Hejazi, An overview and analysis of site remediation technologies, J. Environ. Manage., 71 (2004) 95–122.
[12] A. Parbs, M. Ebert, A. Dahmke, Long-term effects of dissolved carbonate species on the degradation of trichloroethylene by zerovalent iron, Environ. Sci. Technol., 41 (2007) 291–296.
[13] Z. Li, H.K. Jones, R.S. Bowman, R. Helferich, Enhanced reduction of chromate and PCE by pelletized surfactant-modified zeolite/zerovalent iron, Environ. Sci. Technol., 33 (1999) 4326–4330.
[14] D.H. Phillips, T.V. Nooten, L. Bastiaens, M.I. Russell, K. Dickson, S. Plant, J.M.E. Ahad, T. Newton, T. Elliot, R.M. Kalin, Ten year performance evaluation of a field-scale zero-valent iron permeable reactive barrier installed to remediate trichloroethene contaminated groundwater, Environ. Sci. Technol., 44 (2010) 3861–3869.
[15] R.W. Gillham, Enhanced degradation of halogenated aliphaticoarse sand by zero-valent iron, Ground Water, 32 (1994) 958–967.

[16] G.V. Lowry, K.M. Johnson, Congener-specific dechlorination of dissolved PCBs by microscale and nanoscale zerovalent iron in a water/methanol solution, Environ. Sci. Technol., 38 (2004) 5208–5216.
[17] S.R. Rajajayavel, S. Ghoshal, Enhanced reductive dechlorination of trichloroethylene by sulfidated nanoscale zerovalent iron, Water Res., 78 (2015) 144–153.
[18] J. Xu, T. Sheng, Y. Hu. Adsorption–dechlorination of 2,4-dichlorophenol using two specified MWCNTs-stabilized Pd/Fe nanocomposites, Chem. Eng. J., 219 (2013) 162–173.
[19] J. Xu, X. Liu, G.V. Lowry, Z. Cao, H. Zhao, J.L. Zhou, X. Xu, Dechlorination mechanism of 2,4-dichlorophenol by magnetic MWCNTS supported Pd/Fe nanohybrids: rapid adsorption, gradual dechlorination, and desorption of phenol, ACS Appl. Mater. Interfaces, 8 (2016) 7333–7342.
[20] H. Liu, R. Xia, D. Zhao, X. Fan, T. Feng, Enhanced adsorption of 2,4-dichlorophenol by nanoscale zero-valent iron loaded on bentonite and modified with a cationic surfactant, Ind. Eng. Chem. Res., 56 (2016) 191–197.
[21] J. Wan, J. Wan, Y. Ma, M. Huang, Y. Wang, R. Ren, Reactivity characteristics coarse sand of SiO_2-coated zero-valent iron nanoparticles for 2,4-dichlorophenol degradation, Chem. Eng. J., 221 (2013) 300–307.
[22] X. Zhao, W. Liu, Z. Cai, B. Han, T. Qian, D. Zhao, An overview of preparation and applications of stabilized zero-valent iron nanoparticles for soil and groundwater remediation, Water Res., 100 (2016) 245–266.
[23] H. Jia, C. Wang, Adsorption and dechlorination of 2,4-dichlorophenol (2,4-DCP) on a multi-functional organo-smectite templated zero-valent iron composite, Chem. Eng. J., 191 (2012) 202–209.
[24] W. Gao, Y. Zhang, X. Zhang, Z. Duan, Y. Wang, C. Qin, X. Hu, H. Wang, S. Chang, Permeable reactive barrier of coarse sand-supported zero valent iron for the removal of 2,4-dichlorophenol in groundwater, Environ. Sci. Pollut. Res., 22 (2015) 16889–16896.
[25] Y. Tan, J. Liang, G. Zeng, Effects of PRB design based on numerical simulation and response surface methodology, Chin. J. Environ. Eng., 10 (2016) 655–661.
[26] A. Weber, A.S. Ruhl, R.T. Amos, Investigating dominant processes in ZVI permeable reactive barriers using reactive transport modeling, J. Contam. Hydrol., 151 (2013) 68–82.
[27] S.G. Benner, D.W. Blowes, W.D. Gould, R.B. Herbert, C.J. Ptacek, Geochemistry of a permeable reactive barrier for metals and acid mine drainage, Environ. Sci. Technol., 33 (1999) 2793–2799.
[28] H. Deng, W. He, J. Hu, Numerical simulation of Fe0-PRB in rehabilitating groundwater contaminated by nitrate, Chin. Environ. Sci., 35 (2015) 2375–2381.
[29] S.W. Jeen, K.U. Mayer, R.W. Gihham, D.W. Blowes, Reactive transport modeling of trichloroethene treatment with declining reactivity of iron, Environ. Sci. Technol., 41 (2007) 1432–1438.
[30] O. Eljamal, K. Sasaki, T. Hirajima, Numerical simulation for reactive solute transport of arsenic in permeable reactive barrier column including zero-valent iron, Appl. Math. Modell., 35 (2011) 5198–5207.
[31] C. Wanner, S. Zink, U. Eggenberger, U. Mäder, Assessing the Cr(VI) reduction efficiency of a permeable reactive barrier using Cr isotope measurements and 2D reactive transport modeling, J. Contam. Hydrol., 131 (2012) 54–63.
[32] L. Li, C.H. Benson, E.M. Lawson, Modeling porosity reductions caused by mineral fouling in continuous-wall permeable reactive barriers, J. Contam. Hydrol., 83 (2006) 89–121.
[33] K.U. Mayer, D.W. Blowes, E.O. Frind, Reactive transport modeling of an in situ reactive barrier for the treatment of hexavalent chromium and trichloroethylene in groundwater, Water Resour. Res., 37 (2001) 3091–3103.
[34] H. Jia, C. Wang, Adsorption and dechlorination of 2,4-dichlorophenol (2,4-DCP) on a multi-functional organo-smectite templated zero-valent iron composite, Chem. Eng. J., 191 (2012) 202–209.
[35] R. Cheng, J. Wang, W. Zhang, Reductive dechlorination of 2,4-dichlorophenol using nanoscale Fe0: influencing factors and possible mechanism, Sci. China Ser. B: Chem., 50 (2007) 574–579.
[36] J. Xu, J. Tang, S.A. Baig, X. Lv, X. Xu, Enhanced dechlorination of 2,4-dichlorophenol by Pd/Fe-Fe_3O_4 nanocomposites, J. Hazard. Mater., 244 (2013) 628–636.